

## ARTICLES

### Vibrational Spectroscopy of Cyanide-Bridged, Iron(II) Spin-Crossover Coordination Polymers: Estimation of Vibrational Contributions to the Entropy Change Associated with the Spin Transition<sup>†</sup>

Gábor Molnár,<sup>‡,§</sup> Virginie Niel,<sup>||</sup> Ana B. Gaspar,<sup>||</sup> José-A. Real,<sup>||</sup> Antoine Zwick,<sup>⊥</sup>  
Azzedine Bousseksou,<sup>\*,§</sup> and John J. McGarvey<sup>\*,‡</sup>

*School of Chemistry, The Queen's University of Belfast, Belfast BT9 5AG, Northern Ireland, U.K.,  
Laboratoire de Chimie de Coordination, CNRS UPR-8241, 205 route de Narbonne, F-31077 Toulouse, France,  
Departamento de Química Inorgánica, Universidad de Valencia, Avenida Dr. Moliner 50, E-46100 Burjassot,  
Valencia, Spain, and Laboratoire de Physique des Solides, CNRS UMR-5477, 118 route de Narbonne,  
Université Paul Sabatier, F-31062 Toulouse, France*

*Received: February 22, 2002; In Final Form: June 10, 2002*

A series of cyanide-bridged, iron(II) spin-crossover coordination polymers of formula  $\text{Fe}(\text{py})_2[\text{M}(\text{CN})_4]$  ( $\text{M} = \text{Pd}$  or  $\text{Pt}$ ;  $\text{py} = \text{pyridine}$ ) and  $\text{Fe}(\text{pz})[\text{M}(\text{CN})_4] \cdot 2\text{H}_2\text{O}$  ( $\text{M} = \text{Ni}$ ,  $\text{Pd}$ , or  $\text{Pt}$ ;  $\text{pz} = \text{pyrazine}$ ) have been studied by recording the Raman and infrared (IR) spectra of their low-spin (LS) and high-spin (HS) forms in the solid state. Spectral changes upon metal and ligand substitution were used to guide the assignment of vibrational modes. Vibrational entropy changes upon spin transition were analyzed within the harmonic approximation. The results confirm the major contribution of the Fe—ligand vibrations to the overall entropy change associated with the spin transition ( $\sim 60\%$ ), but—contrary to expectations—reveal significant changes in other intra- and intermolecular vibrations, of possible relevance to the high cooperativity of the spin transition.

#### Introduction

Octahedral  $\text{Fe}^{\text{II}}$  spin-crossover (SC) complexes have received much attention from a theoretical point of view, and also because of their possible applications in memory and display devices and as molecular switches.<sup>1,2</sup> Of particular interest for the design of materials with enhanced properties is the understanding of cooperative interactions in the solid state leading to first-order spin transitions accompanied eventually by large hysteresis

loops.<sup>2</sup> Concerning the thermodynamic aspects of SC phenomena, the associated entropy change ( $\Delta S$ ) has been the focus of several experimental and theoretical studies<sup>1d,3</sup> since the original work of Sorai and Seki.<sup>4</sup> These authors pointed out for the first time the importance of this entropy change as controlling the stability of the high-spin (HS) form at high temperature over the (lower enthalpy) low-spin (LS) form. Less well-recognized is the fact that the cooperativity in the solid state may also have an entropic origin, through the anharmonicity of vibrations.<sup>5</sup> Though results on a family of SC compounds appear to indicate a correlation between the cooperativity and the entropy change,<sup>6</sup> the experimental data available so far do not afford a sufficient basis for assessing the validity of this hypothesis.<sup>2a</sup>

Characterization of the vibrational properties of HS and LS forms is central to the above considerations since  $\Delta S$  has a predominantly vibrational origin. Here, a question immediately

<sup>†</sup> The authors dedicate this contribution to Professor François Varret on his 60th birthday.

\* Corresponding authors. E-mail: j.mcgarvey@qub.ac.uk; boussek@lcc-toulouse.fr.

<sup>‡</sup> The Queen's University of Belfast.

<sup>§</sup> CNRS UPR-8241.

<sup>||</sup> Universidad de Valencia.

<sup>⊥</sup> CNRS UMR-5477.

arises as to which vibrational modes are primarily involved. In the case of iron(II) complexes, the increase in the number of the antibonding  $e_g$  electrons upon  $LS(t_2g^6) \rightarrow HS(t_2g^4e_g^2)$  transition weakens significantly the metal–ligand bonds. Thus, the vibrational modes most affected by the change in spin state are, a priori, the metal–ligand stretching and bending frequencies. It is generally assumed that the vibrational entropy stems roughly equally from the six stretching and nine deformation modes associated with the idealized  $FeN_6$  core of the molecule, with other low-frequency intra- and intermolecular or lattice modes having only a minor contribution.<sup>1</sup> Unfortunately, spectroscopic data on which to base consideration of the contributions from different vibrations are rather incomplete. The most extensive studies are those of Takemoto and Hutchinson concerning isotope-substituted  $Fe(phen)_2(NCS/Se)_2$  compounds.<sup>7</sup> Far-IR studies on some other compounds have also been performed.<sup>1b</sup> Recently, these data have been complemented by Raman spectroscopic<sup>8–10</sup> and nuclear inelastic scattering measurements<sup>11</sup> as well as by density functional theory calculations.<sup>8b,11</sup> However, more extensive data are clearly needed in order to calculate more precisely the different vibrational contributions. This, in turn, would lay a firmer basis for improved theoretical treatments incorporating vibrational effects.<sup>5</sup>

In a previous paper,<sup>10</sup> the Raman spectra of  $Fe(phen)_2(NCS)_2$  were analyzed using the assumption of an average frequency representative of the  $FeN_6$  core of the molecule. The results supported the proposition of Sorai and Seki<sup>4</sup> that the intramolecular vibrations represent a primary contribution to the overall entropy change. In a recent paper<sup>9</sup> the inherent limitations of the average frequency approach have been addressed by summing the entropy terms associated with the different vibrational modes. The purpose of the present paper is to further improve this latter approach and to gain a deeper insight into the role of vibrational properties in relation to the spin transition. The systems chosen for study are a group of cyano-bridged, Hofmann-like, coordination polymer compounds (see Figure 1) of formulas  $Fe(py)_2[M(CN)_4]$  ( $M = Pd$  or  $Pt$ ;  $py =$  pyridine) and  $Fe(pz)[M(CN)_4] \cdot 2H_2O$  ( $M = Ni, Pd, \text{ or } Pt$ ;  $pz =$  pyrazine), displaying a variety of  $Fe$ –ligand and other low frequency vibrational modes. The remarkable feature of these complexes is the high cooperativity of the spin transition induced by the network structure and associated with large hysteresis loops. Moreover, the spin transition occurs close to room temperature and is accompanied by a dramatic change of color from orange or yellow (HS form) to garnet (LS form).

## Experimental Section

The samples of coordination polymers were prepared as previously described.<sup>12</sup>

A Spectra Physics 3900 Ti:sapphire laser pumped by an Ar<sup>+</sup> laser (Spectra Physics 2025) was used for Raman excitation at 785 nm. Spectra were recorded by means of a Princeton Instruments CCD detector (LN/UV-1152), coupled to a Jobin-Yvon spectrograph (HR640) with a spectral resolution of 3  $cm^{-1}$ . Raman signals were collected at 180° to the incident laser beam in the 170–2400  $cm^{-1}$  frequency range. The Rayleigh scattering was removed using a holographic notch filter. The pure powder samples were enclosed in the sample holder of an Oxford Instruments Optistat-DN cryostat that allowed the recording of spectra in the vicinity of the spin transition, hence enabling a distinction between temperature and spin-transition effects. To reduce the risk of sample decomposition, laser power was kept low (10 mW) and a cylindrical lens was put between

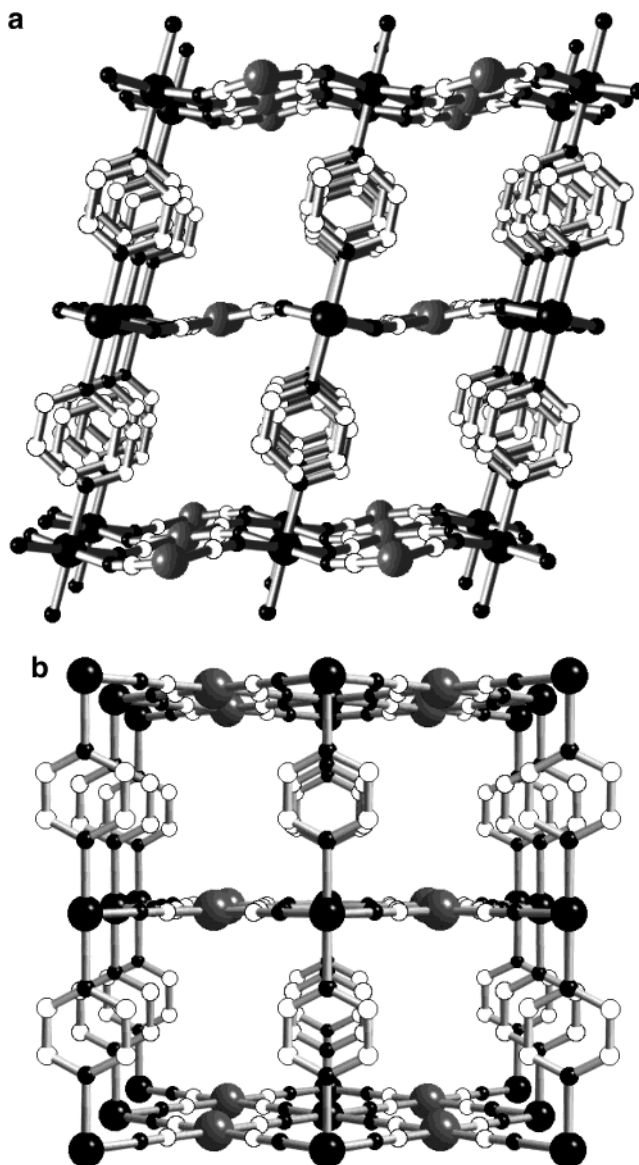


**Figure 1.** Perspective view of the structure of the complexes (a)  $Fe(py)_2[M(CN)_4]$  ( $M = Pd$  or  $Pt$ ) and (b)  $Fe(pz)[M(CN)_4] \cdot 2H_2O$  ( $M = Ni, Pd, \text{ or } Pt$ ).

the laser and the sample. To observe the low-frequency HS modes (below 600  $cm^{-1}$ ), higher laser power (200 mW) was necessary on account of the low signal level. In this case, decomposition problems were avoided by rotating the samples. Spectra close to the laser line (30–310  $cm^{-1}$ ) were acquired using a Dilor XY1800 triplemate spectrograph coupled to a Princeton Instruments CCD detector. In this latter configuration, the 647.1 nm line of a Kr<sup>+</sup> laser (Coherent Radiation Innova) was used as the excitation source with laser power of 10 mW. The exciting radiation was directed through an optical microscope, and the spot was focused on the sample, enclosed in a small liquid nitrogen cryostat, via a  $\times 40$ , long working distance objective. The scattered light was collected in a backscattering configuration, using the same microscope objective, either at room temperature or at 150 K. Owing to the microcrystalline nature of the samples, polarization of the scattered light was not taken into account.

IR spectra of the compounds were recorded using a Perkin-Elmer Spectrum-GX FT-IR spectrometer. It is well-known that SC behavior is considerably influenced by mechanical treatments (e.g., ball-milling);<sup>1</sup> thus several sample preparation methods

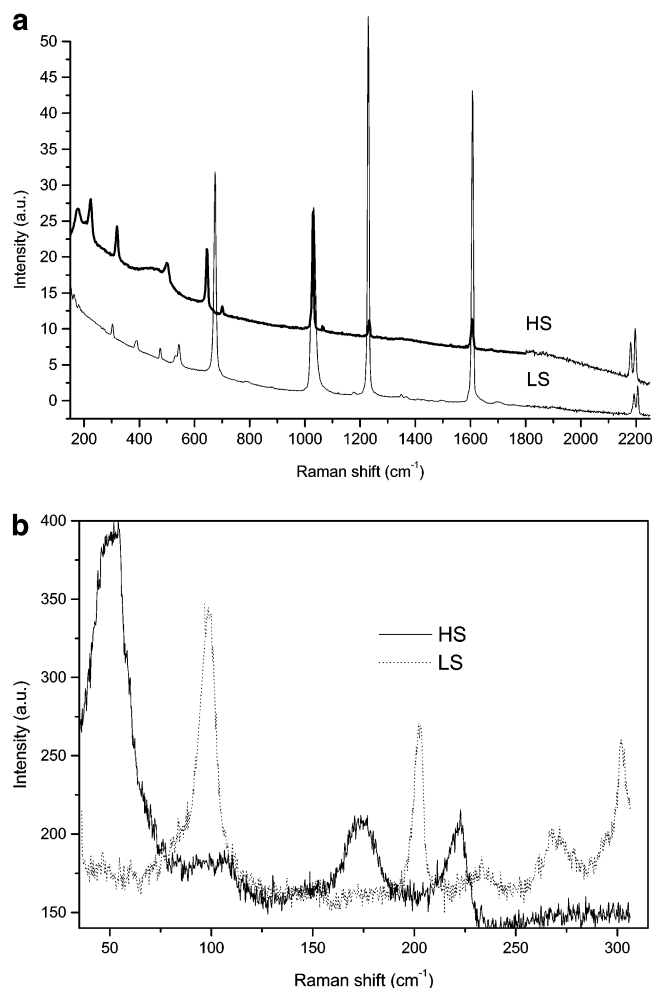


**Figure 2.** (a) Raman and (b) micro-Raman spectra of high- and low-spin Fe(pz)[Pd(CN)<sub>4</sub>]·2H<sub>2</sub>O.

(KBr and polyethylene disks, Nujol mull) were tried with powders either as-received or mortar-crushed. Spectra were taken either at room temperature in the 2500–250 cm<sup>−1</sup> range or at 100 K between 2500 and 400 cm<sup>−1</sup>.

## Results and Discussion

Raman spectroscopy yielded high-quality vibrational data (e.g., see Figure 2 and Figures S (Supporting Information)). No evidence of sample decomposition due to laser irradiation was observed. For all compounds investigated, Raman spectra of the LS isomers were considerably more intense than the HS spectra (by a factor of ~10–20). The spin-transition temperatures observed by Raman spectroscopy corresponded well to the magnetic hysteresis curves.<sup>12</sup> Raman spectra indicated a complete spin transition for the Pd–pz and Pt–pz complexes and an incomplete spin transition for the others, in good accord with the magnetic measurements. In the Ni–pz complex small impurity content was also detected.

On the other hand, IR spectra displaying discernible LS and HS features could only be recorded for the Pd–pz and Pt–pz compounds. IR spectra of crushed powders showed either no or, in some cases, incomplete spin-crossover. For coarse (unground) samples, the IR spectra from the rough, crystalline powders were generally of poor quality. Overall, the vibrational spectra of the complexes proved to be similar with small but significant differences. The main Raman peaks and, where available, those from IR spectra are tabulated in Tables 1–3. Three main groups of vibrational frequencies occur for each

compound. These can be assigned to the CN stretching (around 2200 cm<sup>−1</sup>), internal vibrations of py or pz (between 1700 and 600 cm<sup>−1</sup>), and low-frequency modes below 600 cm<sup>−1</sup> involving mainly metal–ligand vibrations in the cyanide-bridged sheet structure.

**Assignment of Vibrational Modes.** The assignment of CN stretch and ligand modes is relatively easy on the basis of the literature data, but that of the low-frequency modes is more complicated. We recall briefly that the HS crystal structure of the complexes consists of planar, polymeric sheets formed from square-planar M<sup>II</sup>(CN)<sub>4</sub> ions bridged by six-coordinate Fe<sup>II</sup> ions. In the py complexes the neighboring layers are shifted by a symmetry operation of the monoclinic space group (*C*/2*m*),<sup>13</sup> while the structure of the pz derivatives differs in that the bidentate pz ligands bridge the iron atoms; thus no shift between the layers occurs and the space group is tetragonal (*P*4/*m*).<sup>12</sup> In practice, we could find no spectroscopic evidence of significant lattice effects on the symmetry of intramolecular vibrations. Indeed, the vibrations of the py (pz) molecule could be assigned to the molecular group *C*<sub>2*v*</sub> (*D*<sub>2*h*</sub>) by assuming that the selection rules in the crystal are the same as in the isolated state. The remaining vibrations were assigned to the sheet structure having a somewhat idealized point group symmetry of *D*<sub>4*h*</sub>. A similar conclusion has been reached by Akyuz et al. in their study of isostructural py complexes.<sup>14</sup>

The CN stretch, as expected, appears around 2200 cm<sup>−1</sup> as a well-resolved doublet (symmetric and asymmetric stretches) in both Raman and IR spectra (see Table 3). The additional IR activity may result from crystalline state splitting. Compared to the corresponding K<sub>2</sub>M(CN)<sub>4</sub> compounds,<sup>15</sup> ν(CN) modes are shifted to higher frequencies (40–50 cm<sup>−1</sup>), which is a general trend when going from the terminal (M–CN) to the bridging (M–CN–M') cyanide ligands.<sup>16</sup>

Assignment of internal modes of pyridine<sup>17</sup> and pyrazine<sup>18</sup> is fairly straightforward. They appear in the mid-IR region mainly between 600 and 1600 cm<sup>−1</sup> (see Tables 1 and 2). It has long been recognized that the majority of these bands recur on a band-for-band basis in the spectra of their complexes, though discrepancies might occur in the solid state. Compared to the free ligands, a small upward shift of the wavenumbers (0–30 cm<sup>−1</sup>) occurs upon complexation due primarily to kinematic coupling.<sup>16</sup> Larger shifts (ca. 40–70 cm<sup>−1</sup>) are observed only for certain low-frequency modes.

Spectral features below 600 cm<sup>−1</sup> are attributable mainly to metal–ligand vibrations, but their assignment is difficult because of the low signal intensity and the strong coupling between the different modes. However, a major simplifying feature is the apparent absence of internal py and pz bands in this spectral region. It is also known that the “metal-centered” deformation modes—δ(CMC), δ(NFeN)—appear at very low frequencies,<sup>16</sup> usually well below 200 cm<sup>−1</sup>. The large, unresolved spectral features below 100 cm<sup>−1</sup> should be associated mostly with external modes (see Figure 2B). It follows that any mode between 200 and 600 cm<sup>−1</sup> can be attributed without too much uncertainty to coupled vibrations in which the major involvement comes from the ν(Fe–N), ν(M–C), and δ(MCN) modes. Involvement of the latter two mode types should be readily discernible since they would be expected to be very sensitive to the metal (M) substitution. On this basis, several of the features can be assigned as indicated in Table 3 by comparison with the thoroughly analyzed spectra of K<sub>2</sub>M(CN)<sub>4</sub> compounds.<sup>15</sup> Considering now the remaining “FeN<sub>6</sub> modes”, the stretching modes are expected to have the highest frequency. Those that are largely insensitive to the ligand substitution can



**TABLE 1: Main Vibrational Wavenumbers (in  $\text{cm}^{-1}$ ) of Pyrazine in the Compounds  $\text{Fe}(\text{pz})[\text{M}(\text{CN})_4] \cdot 2\text{H}_2\text{O}$  ( $\text{M} = \text{Ni}, \text{Pd}, \text{Pt}$ ) and Their Assignments<sup>a</sup>**

		low-spin form			high-spin form			pyrazine <sup>d</sup>
		Ni	Pd	Pt	Pt	Pd	Ni	
$\nu_{\text{ring}}^c$	$A_g$	1607s	1605s	1608s	1604m	1601m	1603m	1580s
	$A_g$	1031s	1032s	1034s	1028m	1027s	1029s	1016s
	$B_{2g}$						1586w	1525m
$\nu_{\text{ring}}^d$	$B_{1u}$		1486w		1489w		1486w	1483m
	$B_{3u}$		1420m	1418m	1419s	1420s	1416m	1411s
	$B_{3u}$		1177m	1178m	1157m	1157m	1158m	1149s
	$B_{1u}$		1054m	1053m	1053s	1053s	1051s	1018s
$\delta_{\text{CH}}^c$	$A_g$	1230s	1228s	1231s	1231m	1230m	1232m	1233s
	$B_{2g}$	1370w	1368w	1370w				1346w
$\delta_{\text{CH}}^d$	$B_{1u}$		1126w	1126w	1126m	1126m	1128m	1130s
	$B_{3u}$		1087w	1086w	1085m	1086m	1083m	1063s
$\delta_{\text{ring}}^c$	$A_g$	678s	674s	675s	644m	643s	645m	602w
	$B_{2g}$	791w		780w				704s
$\gamma_{\text{ring}}^d$	$B_{2u}$		492m		466sh	466m	468m	418s
$\gamma_{\text{CH}}^d$	$B_{2u}$		826s	827s	804s	806s	803s	785s
combinations			1709m	1710s	1711m	1710m		1694
			1357w	1355m	1357w	1357m		
			1473m	1473m				
nonassigned <sup>d</sup>			552w	555w	528w	528w	1384m	
			1215m		1216s	1216m	723w, 757, 792	

<sup>a</sup> Abbreviations: s, strong; m, medium; w, weak;  $\nu$ , stretching;  $\delta$ , in-plane bending;  $\gamma$ , out-of-plane bending. <sup>b</sup> Taken from ref 18. <sup>c</sup> Observed in Raman spectra. <sup>d</sup> Observed in IR spectra.

**TABLE 2: Main Vibrational Wavenumbers (in  $\text{cm}^{-1}$ ) of Pyridine in the Compounds  $\text{Fe}(\text{py})_2[\text{M}(\text{CN})_4]$  ( $\text{M} = \text{Ni}, \text{Pd}, \text{Pt}$ ) and Their Assignments<sup>a</sup>**

		low-spin form		high-spin form			pyridine <sup>a</sup>
		Pd	Pt	Pt	Pd	Ni <sup>c</sup>	
$\nu_{\text{ring}}^d$	$A_1$	1609m	1607m	1603m	1602w		1580
	$A_1$	1048w	1046w	1039m	1040w		1029
	$A_1$	1019s	1018s	1012s	1012s		992
	$B_1$	1572w	1570w	1574w	1573w		1570
	$A_1$	1488w	1485w				1480
$\nu_{\text{ring}}^e$	$A_1$			1604s	1604s	1604v	1582
	$B_1$			1575	1574w	1575m	1574
	$A_1$			1488	1488m	1487s	1482
	$B_1$			1447	1447s	1446w	1438
	$A_1$			1039	1039s	1038s	1029
$\delta_{\text{CH}}^d$	$A_1$			1011	1011m	1010s	990
	$A_1$	1224m	1222m	1226m	1222w		1218
	$B_1$	1149w	1150m	1151m	1152w		1144
$\delta_{\text{CH}}^e$	$B_1$	1072m	1072m	1070m	1071w		1069
	$A_1$			1220	1220m	1220s	1217
	$B_1$			1153	1153m	1153s	1144
$\delta_{\text{ring}}^d$	$B_1$			1072	1071m	1070s	1069
	$B_1$	651m	650m	653m	652w		652
$\delta_{\text{ring}}^e$	$A_1$	641w	640m		616?		605
	$B_1$			651	651w	651w	652
$\gamma_{\text{ring}}^e$	$A_1$			629	629m	628m	604
	$B_2$	760m	760m	753m	753m	751s	746
$\gamma_{\text{CH}}^e$	$B_2$			420	420	420m	405
	$B_2$			946	946	946m	939
$\gamma_{\text{CH}}^d$	$B_2$			690	690s	689s	
nonassigned <sup>d</sup>		1873w			1872w		

<sup>a</sup> Abbreviations: s, strong; m, medium; w, weak;  $\nu$ , stretching;  $\delta$ , in-plane bending;  $\gamma$ , out-of-plane bending. <sup>b</sup> Taken from ref 17. <sup>c</sup> Taken from ref 14. <sup>d</sup> Observed in Raman spectra. <sup>e</sup> Observed in IR spectra.

be identified as  $\nu(\text{Fe}-\text{N}_{\text{NC}})$  vibrations. The ligand-sensitive bands appearing between 300 and 320  $\text{cm}^{-1}$  can finally be assigned as  $\nu(\text{Fe}-\text{N}_{\text{pz}})$  modes. Table 3 summarizes the findings. While these assignments must remain somewhat tentative at this stage, the spectra are by far the most clear-cut among the spin-crossover complexes studied up to now. It is perhaps surprising that the “separated unit” ( $\text{FeN}_6$ ,  $\text{M}(\text{CN})_4$ , pz, py) approach adopted here applies to such low-frequency vibrations, but the internal consistency of the results gives some confidence that this approach is a reasonable one.

**Spectral Changes upon Spin-Crossover.** The spin transition influences the intensity profiles and is associated with significant frequency shifts in the vibrational spectra of all the complexes investigated. However, since there is no single straightforward hypothesis that could be used to treat intensity changes between the HS and LS entities, the discussion will be confined to consideration of the frequencies alone.

The CN-stretching modes are shifted to higher wavenumbers following the HS to LS transition, similar to the better known NCS complexes, though compared to these, which exhibit  $\nu(\text{CN})$  frequency shifts of 30–50  $\text{cm}^{-1}$  for the HS  $\rightarrow$  LS transition,<sup>1</sup> the corresponding frequency changes here are significantly smaller. The shift is largest in case of the pz complexes (10–15  $\text{cm}^{-1}$ ) and rather less for py complexes (6–7  $\text{cm}^{-1}$ ). A possible origin for this effect might be either enhanced kinematic coupling or subtle changes in the population of N–C orbitals.<sup>1b</sup>

The majority of the low-frequency modes suffer dramatic changes upon spin transition. The general trend is a large decrease of the frequencies when going from the LS to the HS state. As expected, the highest frequency changes (160–180  $\text{cm}^{-1}$ ) are observed for the Fe–N stretching frequencies. These shifts are comparable with values reported for other spin-crossover compounds.<sup>1</sup> Unexpectedly, the  $\delta(\text{NCM})$  vibrations suffer very significant shifts ( $\sim 150 \text{ cm}^{-1}$ ) and the  $\nu(\text{CM})$  modes are also altered considerably (40–60  $\text{cm}^{-1}$ ), indicating that these modes are strongly coupled to the Fe–ligand or lattice modes. By comparison, in the  $\text{Fe}(\text{phen})_2(\text{NCS})_2$  complex the  $\delta(\text{NCS})$  and  $\nu(\text{CS})$  modes are insensitive to the spin change.<sup>8</sup> It is noteworthy also that the external modes suffer important changes too, but these shifts cannot be quantified at present.

The py and pz internal modes are rather insensitive to the spin transition, but some interesting observations can be made. In general, the  $\delta_{\text{CH}}$  modes showed no shift within the measurement error. The observed small frequency shifts ( $\sim 2$ –6  $\text{cm}^{-1}$ ) of the  $\nu_{\text{ring}}$  modes can be understood in terms of a weak kinematic coupling with metal–ligand vibrations. (Temperature effects can be neglected because the HS and LS spectra have been recorded close ( $\pm 20 \text{ K}$ ) to the transition temperature.) Only certain low-frequency modes showed larger frequency changes

**TABLE 3: Main Vibrational Wavenumbers (in cm<sup>−1</sup>) Associated with the Polymeric Sheet Structure in the Complexes and Their Tentative Assignments<sup>a</sup>**

		pyrazine						pyridine				K <sub>2</sub> M(CN) <sub>4</sub> <sup>b</sup>				
		low spin form		Pt	high-spin form			low-spin form		high-spin form		Ni <sup>c</sup>	Pt	Pd	Ni	
		Ni	Pd		Pt	Pd		Ni	Pd	Pt						Pt
$\nu(\text{CN})^d$	A <sub>1g</sub>	2192m	2206m	2216m	2206m	2197m	2182m	2202s	2208s	2202s	2196m		2165	2159	2142	
$\nu(\text{CN})^d$	B <sub>1g</sub>	2183m	2193m	2197m	2183m	2181m	2172m	2188s	2189s	2182s	2181s		2145	2147	2133	
$\nu(\text{CN})^e$	E <sub>u</sub>		2183s	2184s	2172s	2175s	2154m			2171s	2173s	2159s	2134	2134	2127	
hot band?					2147w	2151m	2141m			2145w	2146w	2133w	2123		2121	
$\nu(\text{CM})^d$	A <sub>1g</sub>	528w	543m	580m	~520	502m	486m	538m	572m	496	491		467	424	405	
$\nu(\text{CM})^d$	B <sub>1g</sub>	518w	530m	567m	weak, broad			530m	562m	weak, broad			broad		415	
$\nu(\text{CM})^e$	E <sub>u</sub>		529	~520	503w	504w			~521	505	500	550w	506	485	540	
$\delta(\text{MCN})^d$	E <sub>g</sub>	428w	475m	496m	341m	319m	324m	478w	495m	341m	315m		323	296	303	
$\delta(\text{MCN})^e$	E <sub>u</sub>		~490		464s	421s	438w			460	420	435s	407	383	422	
$\gamma(\text{MCN})^e$	A <sub>2u</sub>		~496		480sh	438sh	444w			479	437	444w	468		443	
$\nu(\text{FeN}_{\text{NC}})^d$	B <sub>1g</sub>	388w	385m	397m	~215sh?			375sh	378w							
$\nu(\text{FeN}_{\text{NC}})^d$	A <sub>1g</sub>	394w	390m	402m	226m	223m	231m	383w	395m	221m	217m					
$\nu(\text{FeN}_{\text{cycle}})^d$	A <sub>1g</sub>	320w	303m	311m	175m	177m	176m			160m	161m					
$\delta(\text{NFeN})^d$	?	215m	203m	211m				189m	191m							
nonassigned <sup>d</sup>		254/264	270w	275w				255w	124w	125w	132/143	132/146				
$\delta(\text{CMC})^d$	B <sub>1g</sub>	105m	105m		105w	105w		100w	100w				95			
combination <sup>d</sup>		2277w		2275w	2249		2246w	2246w	2246w	2246w	2246w					

<sup>a</sup> Abbreviations: s, strong; m, medium; w, weak; sh, shoulder;  $\nu$ , stretching;  $\delta$ , in-plane bending;  $\gamma$ , out-of-plane bending. <sup>b</sup> Taken from ref 15. <sup>c</sup> Taken from ref 14. <sup>d</sup> Observed in Raman spectra. <sup>e</sup> Observed in IR spectra.

**TABLE 4: Measured Relative Frequency Changes ( $\nu_{\text{LS}}/\nu_{\text{HS}}$ ) of Selected Raman Modes upon the Spin Transition and Associated Vibrational Entropy Changes ( $\Delta S_{\text{vib}}^i$  in J K<sup>−1</sup> mol<sup>−1</sup>) Calculated Using Eqs 2 and 3**

mode	Ni-pz		Pd-pz		Pt-pz		Pd-py		Pt-py	
	$\nu_{\text{LS}}/\nu_{\text{HS}}$	$\Delta S_{\text{vib}}^i$	$\nu_{\text{LS}}/\nu_{\text{HS}}$	$\Delta S_{\text{vib}}^i$	$\nu_{\text{LS}}/\nu_{\text{HS}}$	$\Delta S_{\text{vib}}^i$	$\nu_{\text{LS}}/\nu_{\text{HS}}$	$\Delta S_{\text{vib}}^i$	$\nu_{\text{LS}}/\nu_{\text{HS}}$	$\Delta S_{\text{vib}}^i$
$\nu(\text{Fe}-\text{NNC})$	1.71	3.7	1.75	3.6	1.78	3.6	1.76	3.4	1.75	3.3
$\nu(\text{Fe}-\text{N}_{\text{cycle}})$	1.82	4.4	1.71	3.8	1.78	4.0				
$\delta(\text{MCN})$	1.32	1.8	1.49	2.2	1.45	1.8	1.52	2.0	1.45	1.6
$\nu(\text{M}-\text{C})$	1.09	0.38	1.08	0.33	1.11	0.37	1.09	0.30		
$\delta(\text{ring})$	1.05	0.19	1.05	0.14	1.05	0.11	1.04	0.08		
$\nu(\text{ring})^a$	1.002	~10 <sup>−3</sup>	1.005	~10 <sup>−3</sup>	1.006	~10 <sup>−3</sup>	1.007	~10 <sup>−4</sup>	1.007	~10 <sup>−4</sup>
$\nu(\text{N}-\text{C})$	1.005	~10 <sup>−4</sup>	1.004	~10 <sup>−5</sup>	1.004	~10 <sup>−5</sup>	1.004	~10 <sup>−6</sup>	1.004	~10 <sup>−6</sup>
$T_c$	292		250		230		210		212	
$\Delta S_{\text{vib}}(\text{total})^b$	55 <sup>d</sup>		70		75		55		57	
$\Delta S_{\text{vib}}(\text{FeN}_6)^c$	47 ± 15		42 ± 18		44 ± 18					

<sup>a</sup> 1030 cm<sup>−1</sup> mode for pz complexes, 1015 cm<sup>−1</sup> mode for py complexes. <sup>b</sup> Calculated by eq 1 using  $\Delta S$  data (extrapolated at 100% of spin conversion) from ref 12. <sup>c</sup> Estimated vibrational entropy change associated with the FeN<sub>6</sub> core (see text for details of calculation). <sup>d</sup> Ill-determined due to impurities.

(10–30 cm<sup>−1</sup>) upon spin transition. This behavior can be explained by the coupling of these modes to various Fe–N vibrations.<sup>17,18</sup> It should be noted that in the Fe(phen)<sub>2</sub>(NCS)<sub>2</sub> complex the  $\delta_{\text{ring}}$  modes showed similar changes.<sup>8</sup>

Data in Tables 1–3 reveal also that the frequency shifts upon HS to LS transition are often similar to those observed when the spectra of pure ligands and their complexes are compared. Bayer and Ferraro noted that the vibrational spectra of pyrazine under pressure show similarities to the corresponding spectra of its metal complexes.<sup>19</sup> They suggested that this might indicate that complexation involves an “internal pressure effect”. Following this idea in the present instance, it might be suggested that such a “pressure effect” is enhanced upon the HS to LS transformation, leading to further shift in the frequencies of various ligand modes (pz, py, and also M(CN)<sub>4</sub>). In this context, it is also worth mentioning that the frequencies of C–N, C–M, and Fe–N stretches as well as the lattice vibrations are systematically higher in the pz complexes compared to the py complexes (both HS and LS forms). This could also be explained by an internal pressure effect arising from the more rigid three-dimensional structure of the pz complexes. Such an internal pressure could also be responsible for the higher transition temperature (see Table 4) of the pz complexes.

**Entropy Changes upon Spin-Crossover.** Bearing in mind the somewhat tentative nature of the above assignments, estimation of the entropy changes associated with the different

vibrations will now be considered. The entropy change upon spin transition can be represented as the sum of electronic, vibrational, configurational, rotational, and translational terms. The two latter are effectively excluded from consideration in the solid state. Moreover, in the absence of orientational disorder the configurational term can also be neglected. The electronic term may contain contributions from both spin and orbital degeneracy. For octahedral iron(II) spin-crossover complexes (<sup>1</sup>A<sub>1g</sub> → <sup>5</sup>T<sub>2g</sub>), the orbital degeneracy is usually removed; thus the electronic entropy may be obtained directly from the spin-multiplicity change as 13.4 J K<sup>−1</sup> mol<sup>−1</sup>.<sup>4</sup> On the other hand, the measured overall entropy change for these complexes varies between 68 and 85 J K<sup>−1</sup> mol<sup>−1</sup>,<sup>12</sup> where the “missing” entropy is thought to be of vibrational origin:

$$\Delta S_{\text{vib}} \cong \Delta S - \Delta S_{\text{el}} \quad (1)$$

In the harmonic approximation, the vibrational entropy of an oscillator  $i$  of frequency  $\nu$  (s<sup>−1</sup>) can be expressed as follows:<sup>10</sup>

$$S_{\text{vib}}^i = k[\Omega \tanh(\Omega) - \ln(2 \sinh(\Omega))] \quad (2)$$

where  $\Omega$  equals  $h\nu/2kT$ . The entropy change of the  $i$ th oscillator upon the spin-transition can be obtained simply by

$$\Delta S_{\text{vib}}^i = S_{\text{vib}}^i(\nu_{\text{HS}}, T_c) - S_{\text{vib}}^i(\nu_{\text{LS}}, T_c) \quad (3)$$

where the transition temperature  $T_c$  is defined by  $\Delta G(T_c) = 0$ .

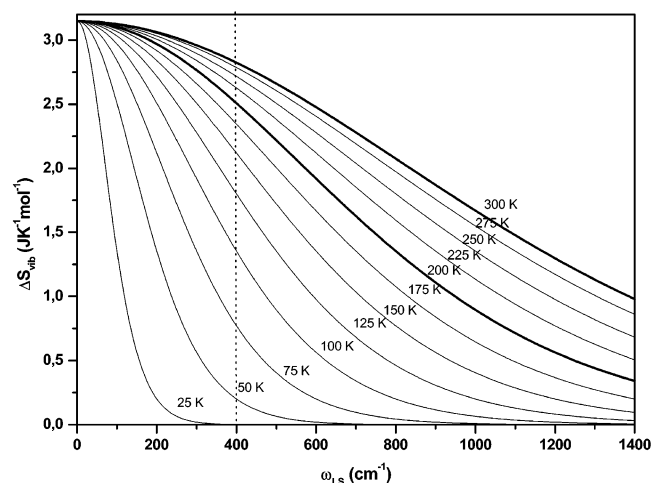


**Figure 3.** Vibrational entropy change upon spin transition as a function of the vibrational wavenumber. The curves were calculated for a unique mode using eqs 2 and 3 with  $\nu_{\text{HS}} = \nu_{\text{LS}}/1.5$  for different values of  $T_c$  between 25 and 300 K. Highlighted in bold is the  $T_c$  range of the complexes under study.

Using eqs 2 and 3 we have calculated the contribution of some selected vibrational modes to  $\Delta S_{\text{vib}}$  (see Table 4). Of special interest is the entropy change associated with the 15 vibrations of the idealized  $\text{FeN}_6$  core. As explained in ref 10, a complete determination cannot be expected even from a variety of experimental and theoretical sources. However, reasonable estimates can be obtained either by using an average frequency in eq 2<sup>10</sup> or by summing up the  $S_{\text{vib}}^i$  contributions over the observed modes and applying an appropriate weighting for the unknown ones.<sup>9</sup> While the former method has the advantage of not requiring the assignment of individual modes, it will, at best, give a gross approximation. On the other hand, the summation method can provide a fairly good estimation even if several modes remain unknown provided that the entropy varies smoothly over the appropriate frequency range.

Indeed, as shown in Figure 3, the vibrational entropy is a relatively “smooth” function of the frequency between 0 and 400  $\text{cm}^{-1}$  if  $T_c$  is as high as in the case of the present group of complexes. In other words, in this low-frequency/high-temperature limit any change in entropy can be unambiguously attributed to shifts in vibrational frequencies because the population of vibrational modes is no longer frequency-dependent within the implied range.<sup>20</sup> The vibrational entropy changes associated with the  $\text{FeN}_6$  core are reported in Table 4 for the pz complexes, which allow for a more reliable estimation.<sup>21</sup> The corresponding error bars are determined mostly by the fact that the relative frequency changes of the unknown  $\text{FeN}_6$  modes ( $\nu_{\text{LS}}/\nu_{\text{HS}}$ ) may differ from those of the assigned modes. However, an upper and a lower limit for  $\nu_{\text{LS}}/\nu_{\text{HS}}$  associated with the  $\text{FeN}_6$  modes can be established. The upper limit ( $\sim 1.75$ ) is given by the symmetric Fe–N stretching mode, which is known to be the most affected by the spin state change.<sup>1</sup> A reasonable lower limit ( $\sim 1.5$ ) is effectively set by the  $\delta(\text{NCM})$  mode, which is expected to be less influenced by the spin change of the  $\text{Fe}^{\text{II}}$  ion. Using these limits, one can estimate the error incurred in applying the weighting method (see Figure 4). Clearly, this error must remain relatively large at this stage (see Table 4), with a significant reduction depending on more firmly based band assignments, e.g., by means of isotopic substitution.

Notwithstanding the approximations inherent in the data of Table 4, the results show clearly that the main contribution to the vibrational entropy change comes from the  $\text{FeN}_6$  core vibrations ( $60 \pm 20\%$ ), but also that other modes make a

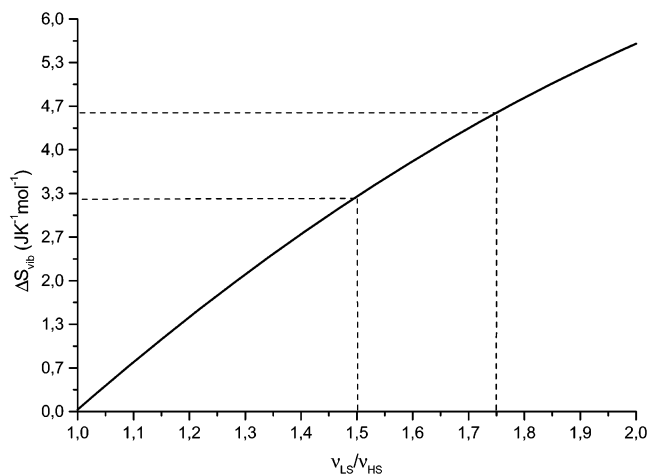


**Figure 4.** Vibrational entropy change upon spin transition as a function of the relative frequency change. The curve was calculated for a unique mode using eqs 2 and 3 with  $\omega_{\text{LS}} = 200 \text{ cm}^{-1}$  and  $T_c = 290 \text{ K}$ . (See text for the meaning of the dotted lines.)

significant contribution. The influence of internal pz and py modes is negligible ( $<1\text{--}2\%$ ). Taking into account the relatively large entropy changes associated with the  $\text{M}(\text{CN})_4$  modes ( $\sim 10\%$  for the 13 modes detected out of 24<sup>22</sup>), a large part of the remaining entropy change can reasonably be attributed to the  $\text{M}(\text{CN})_4$  modes. However, one should not forget that these modes are—in all probability—strongly coupled to the metal–ligand vibrations. Therefore, one could interpret the frequency and related entropy changes either by assuming a mechanical coupling to the Fe–N bonds or by changes in the force field of the  $\text{M}(\text{CN})_4$  moiety. Isotope substitution and high-pressure experiments could help to clarify the extent to which these two mechanisms account for the observed shifts.

## Conclusions

The primary goal of this work was to try to address the shortcomings of the mean-frequency approach<sup>10</sup> for estimating the various contributions to the vibrational entropy change associated with the SC phenomenon. Although the need to study complexes where the low frequency vibrational spectra can be more or less completely assigned does severely restrict the range of systems for investigation, the family of high-symmetry complexes studied here does meet the requirements very well. We have also identified another important feature of these complexes in this respect: their high  $T_c$  value. As a consequence, they satisfy closely the high-temperature limit, which enables compensatory weighting, within acceptable error limits, for any undetected modes. While the present results provide more comprehensive support than previously available for the now generally accepted idea<sup>1</sup> that the main contribution to the entropy change comes from the  $\text{Fe}^{\text{II}}$ –ligand vibrations, the findings also appear to indicate that other intra- and intermolecular vibrations can make nonnegligible contributions as well. We believe that these complexes represent an appropriate platform from which to gain a deeper insight into the interesting vibronic properties of SC solids. Pressure tuning and isotope substitution studies are under way to explore these possibilities.

It is somewhat surprising that until now relatively little attention has been paid to the effects of SC on ligand or intermolecular vibrational modes, particularly in relation to the phenomenon of cooperativity. The present group of complexes provides the first significant opportunity to do so. Metal dilution studies could throw further light on the nature of the cooperative

interactions. Finally, this study serves also to highlight the inherent advantage of modern Raman spectroscopy (involving no sample grinding) over IR spectroscopy for the study of spin-crossover phenomena and suggests that future spin-crossover research should focus more on this technique.

**Acknowledgment.** This work was supported by the European Community TMR Network TOSS (ERB-FMRX-CT98-0199). G.M. acknowledges EC support through a Marie Curie Fellowship (Project MCFI 2000-01835).

**Supporting Information Available:** Raman spectra of coordination polymer samples. This material is available free of charge via the Internet at <http://pubs.acs.org>.

## References and Notes

- (1) (a) Gütlich, P.; Hauser, A.; Spiering, H. *Angew. Chem., Int. Ed. Engl.* **1994**, *33*, 2024. (b) Gütlich, P. *Struct. Bonding (Berlin)* **1981**, *44*, 83. (c) Goodwin, H. A. *Coord. Chem. Rev.* **1976**, *18*, 293. (d) König, E. *Struct. Bonding (Berlin)* **1991**, *76*, 51.
- (2) (a) Kahn, O. *Molecular magnetism*; Wiley-VCH: New York, 1993. (b) Kahn, O.; Martinez, C. J. *Science* **1998**, *279*, 44. (c) Real, J. A.; Andrés, E.; Munoz, M. C.; Julve, M.; Granier, T.; Bousseksou, A.; Varret, F. *Science* **1995**, *268*, 265. (d) Gütlich, P.; Garcia, Y.; Woike, T. *Coord. Chem. Rev.* **2001**, *219–221*, 839.
- (3) (a) Jakobi, R.; Spiering, H.; Gütlich, P. *J. Phys. Chem. Solids* **1992**, *53*, 267. (b) Nakamoto, T.; Tan, Z. C.; Sorai, M. *Inorg. Chem.* **2001**, *40*, 3805.
- (4) Sorai, M.; Seki, S. *J. Phys. Chem. Solids* **1974**, *35*, 555.
- (5) (a) Bousseksou, A.; Constant-Machado, H.; Varret, F. *J. Phys. (Fr.)* **1995**, *5*, 747. (b) Zimmermann, R.; König, E. *J. Phys. Chem. Solids* **1977**, *38*, 779.
- (6) Capes, L.; Létard, J. F.; Kahn, O. *Chem. Eur. J.* **2000**, *6*, 2246.
- (7) Takemoto, J. H.; Hutchinson, B. *Inorg. Chem.* **1973**, *12*, 705.
- (8) (a) Dennis A. C. Ph.D. Thesis, The Queen's University of Belfast, UK, 2000. (b) Hoefer, A. Ph.D. Thesis, University of Mainz, Germany, 2000.
- (9) Moliner, N.; Salmon, L.; Capes, L.; Carmen Munoz, M.; Letard, J. F.; Bousseksou, A.; Tuchagues, J. P.; McGarvey, J. J.; Dennis, A. C.; Castro, M.; Burriel, R.; Real, J. A. *J. Phys. Chem. B* **2002**, *106*, 4276.
- (10) Bousseksou, A.; McGarvey, J. J.; Varret, F.; Real, J. A.; Tuchagues, J. P.; Dennis, A. C.; Boillot, M. L. *Chem. Phys. Lett.* **2000**, *318*, 409.
- (11) (a) Paulsen, H.; Winkler, H.; Trautwein, A.; Grunsteudel, H.; Rusanov, V.; Toftlund, H. *Phys. Rev. B* **1999**, *59*, 975. (b) Paulsen, H.; Benda, R.; Herta, C.; Schünemann, V.; Chumakov, A. I.; Duellund, L.; Winkler, H.; Toftlund, H.; Trautwein, A. X. *Phys. Rev. Lett.* **2001**, *86*, 1351.
- (12) Niel, V.; Martinez-Agudo, J. M.; Munoz, M. C.; Gaspar, A. B.; Real, J. A. *Inorg. Chem.* **2001**, *40*, 3838.
- (13) Kitazawa, T.; Gomi, Y.; Takahashi, M.; Takeda, M.; Enomoto, M.; Miyazaki, A.; Enoki, T. *J. Mater. Chem.* **1996**, *6*, 119.
- (14) Akyuz, S.; Dempster, A. B.; Morehouse, R. L.; Suzuki, S. *J. Mol. Struct.* **1973**, *17*, 105.
- (15) Kubas, G. J.; Jones, L. H. *Inorg. Chem.* **1974**, *13*, 2816.
- (16) Nakamoto, K. *Infrared and Raman spectra of inorganic and coordination compounds*; John Wiley & Sons: New York, 1986.
- (17) Kantarci, Z.; Bayrak, C.; Bayar, S. *J. Mol. Struct.* **1997**, *407*, 155.
- (18) Zarembowitch, J.; Bokobza-Sebagh, L. *Spectrochim. Acta, Part A* **1976**, *32*, 605.
- (19) Bayer, R.; Ferraro, J. R. *Inorg. Chem.* **1969**, *8*, 1654.
- (20) Note that the "high-temperature limit" does not refer here to the classical high-temperature approximation:  $S_{\text{vib}} = -k \ln(h\nu/kT)$ . Throughout our calculations we used eq 2 to calculate  $S_{\text{vib}}$ .
- (21) Overall, 15 vibrations can be associated with the idealized FeN<sub>6</sub> core. To determine the number of unknown modes, the degeneracy of the identified FeN<sub>4</sub>N'<sub>2</sub> modes have been considered by assuming  $D_{4h}$  symmetry.
- (22) Calculated for the Pd–pz complex assuming  $D_{4h}$  symmetry.